STUDIES WITH A SMALL GAMELAN GONG

R Perrin Institute for Fundamental Sciences, Massey University, Palmerston North, NZ
S Hamdan Faculty of Engineering, Universiti Malaysia Sarawak (UNIMAS), Malaysia
B Halkon Wolfson School of Mechanical and Manufacturing Engineering, Loughborough University, Loughborough, UK
GM Swallowe Department of Physics, Loughborough University, Loughborough, UK

1 INTRODUCTION

A gamelan is an ensemble of ethnic musical instruments from parts of Indonesia where it is central to musical art and commands huge respect. It is also found in some neighboring countries. While it involves many different types of instruments its backbone consists of metalophones and gongs.

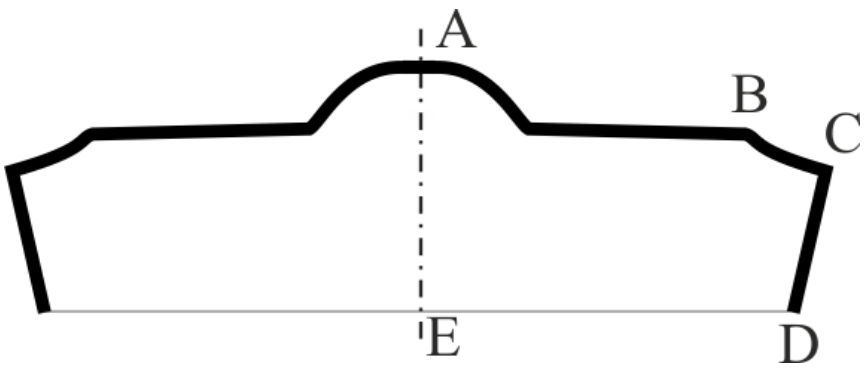

Figure 1. Vertical cross-section through a small gamelan gong

Gamelan gongs come in a wide range of sizes but all are of similar general structure. In Figure 1 we show a vertical cross-section through the centre of a typical small gamelan gong placed on a horizontal surface. It consists of a central dome A on top of a flat plate which is terminated by a shoulder BC and then a deep inward sloping rim CD. The vertical line AE is the axis of symmetry. These gongs are rung by being stuck on the central dome with a mallet. Large gongs are suspended vertically by strings. Smaller ones are mounted horizontally from underneath on parallel strings. Since a "perfect" gong has complete axial symmetry one can conclude[1] that its normal modes have nodal patterns consisting of m equally spaced "diameters" and n circles parallel to the rim's edge. Modes with m = 0 are axisymmetric singlets while those with $m > 0$ occur in degenerate pairs with the diameters of one bisecting those of its partner. Modes can be designated by (m, n) with the addition of a subscript outside the brackets if it is desired to distinguish between a doublet's components. In practice gamelan gongs are cast, sometimes rather roughly, and so have geometrical and metallurgical imperfections which break the basic axial symmetry. Consequently the doublets split and distortions appear in some nodal patterns. In the present work we are concerned with a small steel gong of 20.7cm diameter originating from Sarawak.

In an earlier study with the same gong[2] we produced an axially symmetric finite-element model (FEM) and compared its predictions with experimental results obtained using Electronic Speckle Pattern Interferometry (ESPI). We now report an extension of this study using Scanning Laser Doppler Vibrometry (SLDV) using a mounting method which better simulates that used in practice.

2 PREVIOUS RESULTS

Unfortunately the optical system used in the previous ESPI study did not permit the gong to be supported horizontally, as it would have been during normal playing. Instead it was suspended vertically from a clamp attached to the top of the rim. This would certainly have influenced some of the modes so it was incorporated into the FEM, breaking the model's axial symmetry and resulting in some of the predicted doublets being split.

A comparison of the FEM and ESPI results was not a straightforward matter because the real gong proved to have significant non-linear properties manifesting themselves in the forms of both harmonics and sub-harmonics of true modes. There were also serious distortions of some nodal patterns, especially for cases with n > 1. Initially the experiments were performed looking at the top plate along the symmetry axis. This proved insufficient because, for modes with n = 0, no nodal patterns were observed on the top plate for m > 2. To observe these patterns it was necessary to look at the rim from a direction normal to the symmetry axis. When this was done (m, 0) modes with m up to 10 were readily identified. The reason for this was that, for m ≥ 2, going radially across the top plate, there exists a critical point inside which the motion is evanescent[3]. This point moves ever further away from the symmetry axis as m increases, resulting in modes being observable only on the rim.

Modes with n = 1 were relatively easy to identify because their single nodal circle occurred at or close to the inner edge of the shoulder. Although evanescence was still present the amplitudes did not become undetectably small until the central dome was reached. While a few modes with n > 1 were identified, this became increasingly problematical as n increased. We therefore paid them relatively little attention.

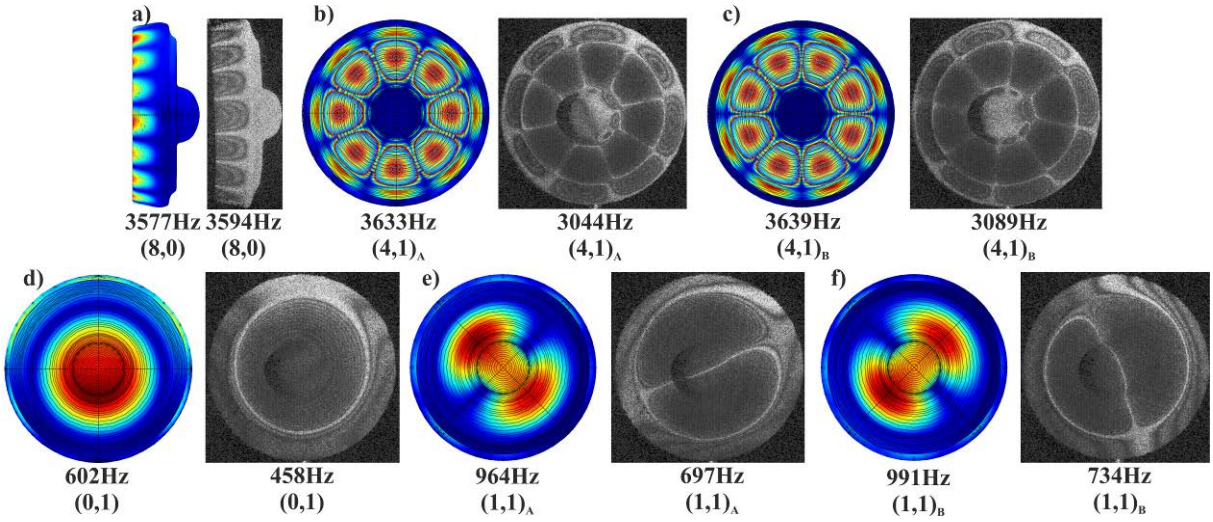

Figure 2. Modes predicted by FEM and the corresponding Interferograms obtained using ESPI.

Figure 2 shows examples of interferograms obtained using ESPI together with the corresponding FEM results. Clearly the modal forms are in good agreement. In the first row are an n = 0 "rim" mode plus an orthogonal pair of n = 1 "plate" modes. In the second row are a (singlet) m = 0 axisymmetric mode and an orthogonal pair of m = 1 modes. It should be noted that only m = 0 and m = 1 modes are free from evanescent behaviour as one moves towards the symmetry axis.

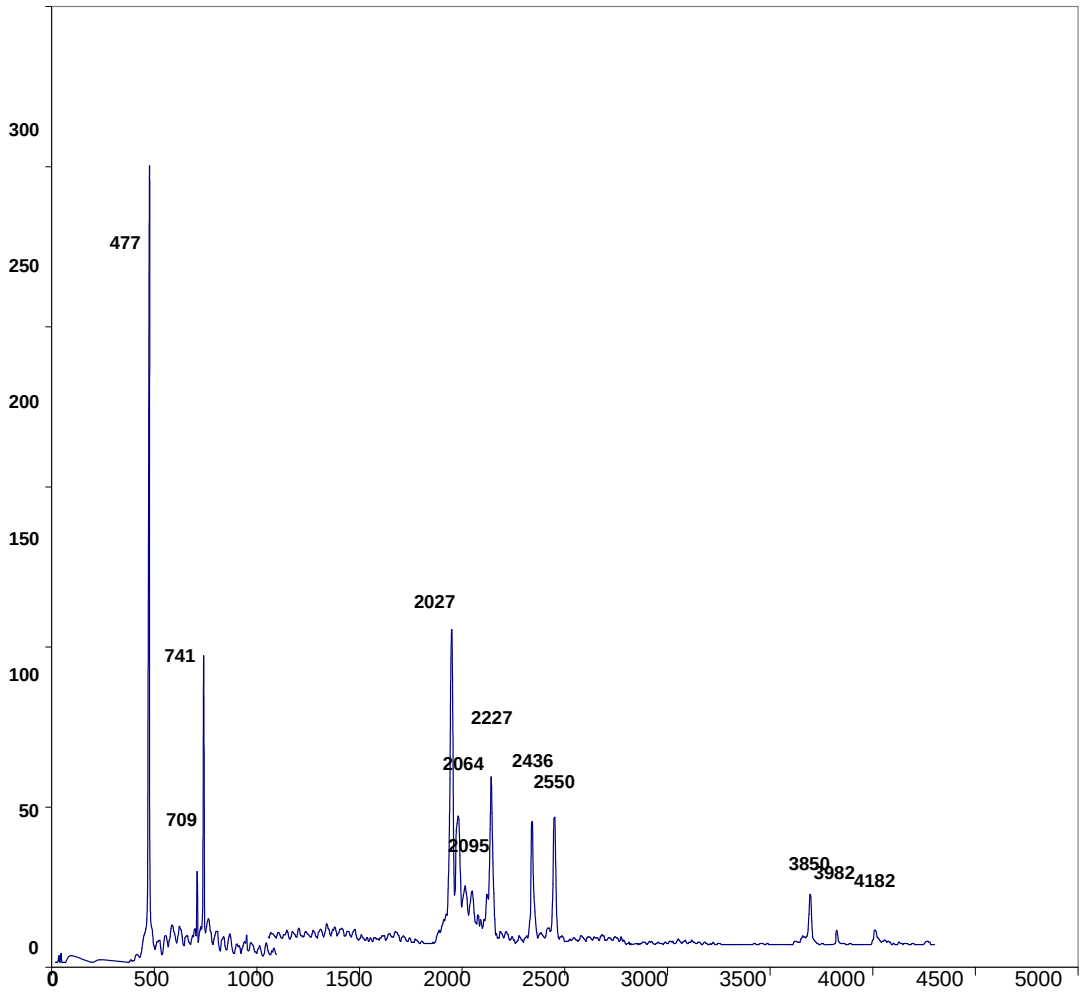

Figure 3. Time-averaged acoustic power spectrum

Taking a time-averaged acoustic power spectrum of the gong, after striking it on the dome, revealed, not surprisingly, that the singlet (0,1) mode was by far the most important. This can be seen in Figure 3. The pairs of (1,1) and (2,1) modes were also significant. Only modes with n = 1 and some of their (non-linear) harmonics made worthwhile contributions. We found no evidence of a second important axisymmetric mode contributing as reported by Rossing[4] using a different gong. It is possible that he was seeing a subharmonic of the (0,1).

The frequency predictions of the FEM and the corresponding ESPI measurements are shown in Figures 4 and 5 for n = 0 and n = 1 respectively. Frequencies above 5000 Hz are excluded because of the problems of interpretation of the ESPI forms. Because the n = 0 “rim” pairs were significantly split we show, for the sake of clarity, the higher frequency components only. Clearly the agreement is excellent. In the case of n = 1 “plate” modes we have again shown only the higher frequency components. In this case the agreement was not nearly so good although the trends are identical. To emphasize this we have reduced the FEM predictions by 20% in the graph. Such a deviation could easily be due to the variations of the thickness of the plate, from casting, making the model too crude an approximation. The n = 0 modes hardly depend at all on the details of the plate but rather on the details of the rim geometry. Higher n values have been excluded from the graphs because of the problems involved in the identification of their interferograms.

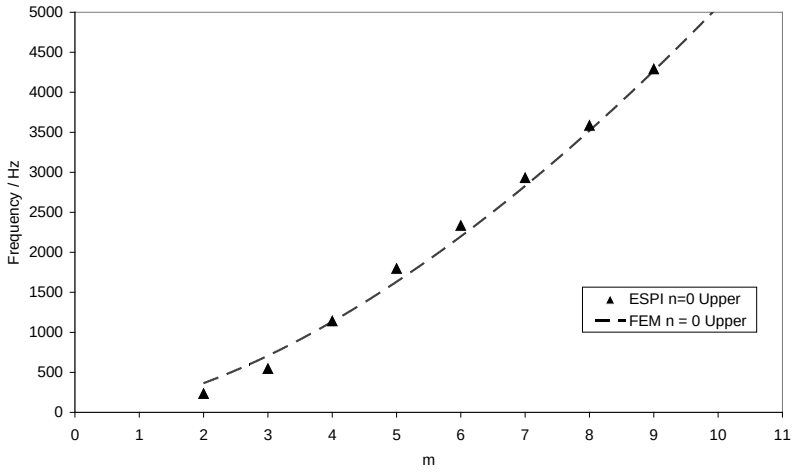

Figure 4. Frequency v m for ESPI and FEM for n = 0 (upper component**)**

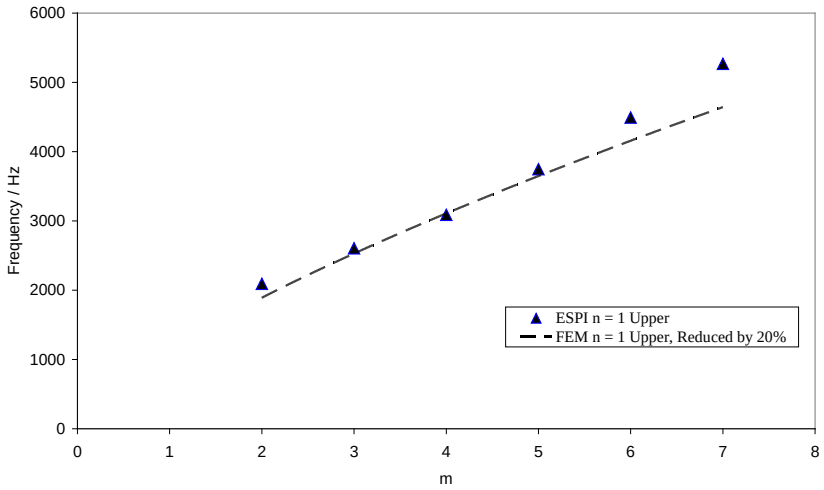

Figure 5. Frequency v m for ESPI and FEM for n = 1 (upper component**)**

3 NEW INVESTIGATIONS

In order to check our previous results which were obtained using rigid clamping at one point it was decided to conduct a new set of investigations on the same gamelan gong but now using Scanning Laser Doppler Vibrometry (SLDV). This technique, now utilised in a number of sectors as an alternative to traditional contact vibration measurement techniques involves the scanning of a laser beam across the surface of the structure of interest using a pair of orthogonally aligned mirrors. Because the method measures velocity in the direction of the laser beam, and this was directed towards the gong parallel to the axis of symmetry, we were only able to study motion in this direction. Simultaneous direct observations of the rim were not possible

.

3.1 Experimental Details

The gamelan gong was suspended on a compliant mounting with sufficiently low stiffness for the rigid body modes to occur at frequencies an order of magnitude lower than the lowest dynamic natural frequency. A driving point on the structure was chosen such that there was expected to be activity in all the modes of interest and a miniature force transducer (B&K Type 8203) attached to measure the (reference) input signal. Excitation was generated using an LDS V101 permanent magnet electrodynamic shaker which was similarly lightly suspended, in this case with bungees, and connected to the force transducer through a pin vice and thin wire “stinger” arrangement. The stinger, being rigid in the direction of excitation but flexible in the other directions, ensured that any local mass and stiffness modifications to the gong were minimised. Consequently the determined natural frequencies were expected to be close to those that would be obtained with acoustic excitation.

A Polytec PSV300 (2D) SLDV system was used to measure the response of the gong when subjected to a broadband (white noise) excitation. The excitation signal was generated within the SLDV electronics, with a range equivalent to the specified frequency range of interest of the acquisition system, and amplified using an LDS PA25E power amplifier. A burst of random excitation was used with a 5% of block-length build-up and a 50% of block-length burst. These parameters were found to lead to gong response that decayed within the acquisition block such that a rectangular acquisition window could be used without risk of leakage and a corresponding increase in the damping ratio determined. 20 linear averages were used to maximise the signal-to-noise ratio in the measured mobility Frequency Response Functions (FRF’s). The coherence function was interrogated to confirm strong signal-to-noise ratio in the region of interest.

Response measurements were directly defined in the SLDV software on a regular polar grid with sufficient spatial resolution of measurement points to enable representation of the mode shapes at all frequencies of interest. The SLDV, was positioned five metres from the gong in order that the angle of incidence of the laser beam was never more than 5 degrees off axis (and therefore such that sensitivity to velocity components orthogonal to the symmetry axis was negligible). The user interface readily identifies the measurement points at which an FRF has been captured successfully and those at which it has not. Occasionally, if the background light, which has the form of a laser speckle pattern because the surface is rough on the scale of the laser wavelength[6], is consistently reduced in amplitude, it may be necessary to adjust slightly the alignment of the device or adjust the response point to enable measurement. The frequency range of interest and required specified settings often led to acquisition periods of several hours; care was taken to ensure that the ambient conditions and other environmental effects did not impact significantly on the quality of the measured data.

(Modal) processing of the FRF’s was performed in the Polytec Scanning Vibrometer software by manually defining multiple (search) frequency bands within the sum FRF from which the peak amplitudes were automatically identified. A Least Squares Complex Exponential curve-fitting algorithm was subsequently used to synthesise a number of single degree of freedom damped exponentials from which the Eigenfrequency and damping ratio were extracted.

3.2 Experimental Results

Figure 6 shows a selection of the modal forms generated by SDLV. When the top row is compared with that of Figure 2 the agreement for the (4,1) modes is seen to be striking, except that SDLV shows relatively little motion on the shoulder. This could be attributed to the fact that, as previously described, SDLV measures velocity in the direction of the laser beam and, given the geometry of the gamelan gong the shoulder motion will be much more significant in directions not closely aligned with the incident laser beam direction. The forms shown in the second rows are in, perhaps,

even better agreement. In this case there is little shoulder motion expected. In the third row of Figure 6 we include members of the (2,0) and the (2,1) pairs in order to emphasise the differences between them.

Comparing the spectra in Figures 7 and 3 one sees a good overall agreement between the modal frequencies although, as expected, the relative magnitudes of the peaks differ. Also the SLDV spectrum shows up the (4,1) modes which do not appear in the acoustic spectrum, although they were easily detected by ESPI. Table 1 shows a comparison of the frequencies measured acoustically with those from ESPI and SLDV. Overall the agreement between ESPI and SLDV is good, although SLDV detected far fewer modes.

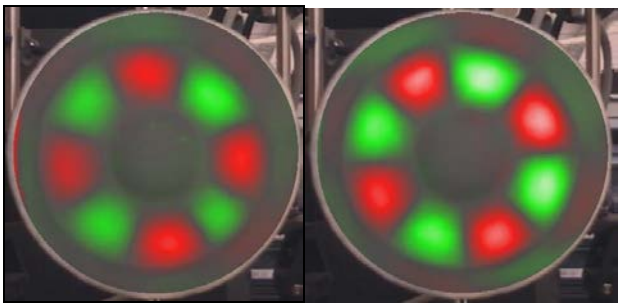

3008Hz $(4,1)_A$ 3073 Hz $(4,1)_B$

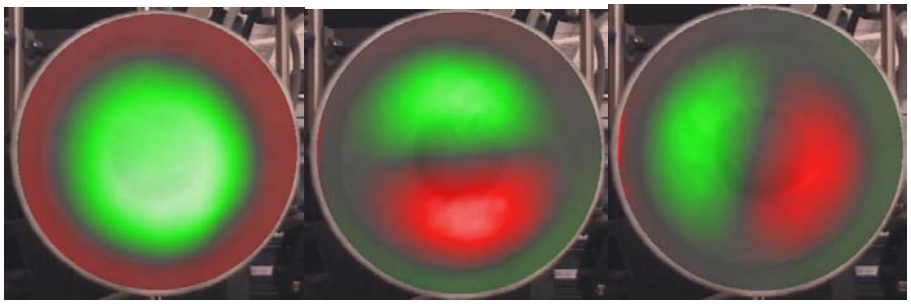

420Hz (0,1) 723Hz $(1,1)_A$ 786Hz $(1,1)_B$

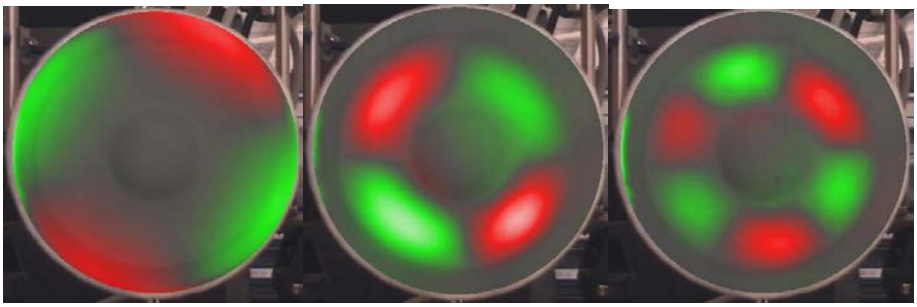

516Hz $(2,0)_A$ 1986Hz $(2,1)_A$ 2556Hz $(3,1)_B$

Figure 6. Selected modal patterns of the gong obtained by SLDV

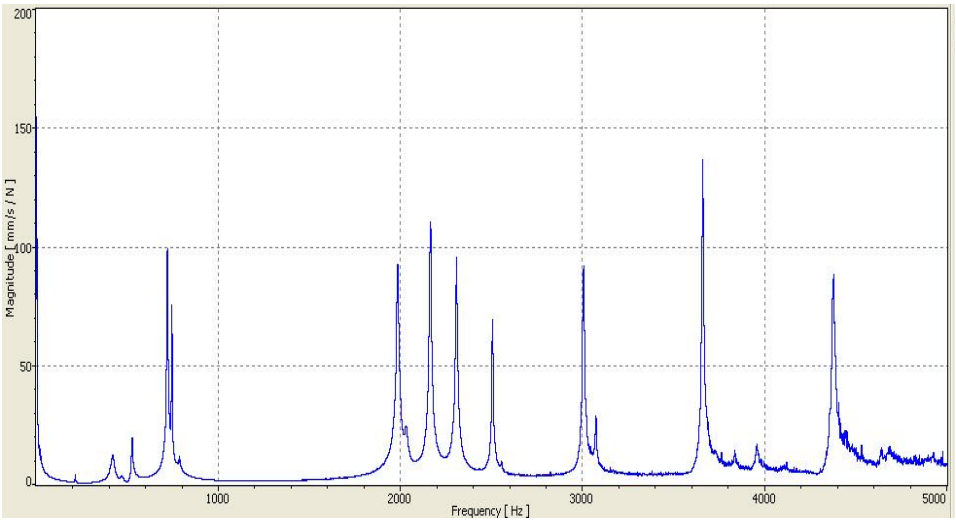

Figure 7. SLDV spectrum for the gong

modes	ESPI (Hz)	SLDV (Hz)	Acoustic (Hz)
(0,1)	458	420	477
(1,1)	698,734	723, 786	709, 741
(2,1)	2005, 2093	1986, 2081	2027, 2064
(3,1)	2529, 2606	2506, 2556	2436, 2550
(4,1)	3089, 3633	3008, 3073	---, ---
(5,1)	3726, 3748	3661, ---	3850, 3982
(6,1)	4469, 4494	---, ---	---, ---
(1,0)	69, 99	---, ---	---, ---
(2,0)	240, 244	216, ---	237, ---
(3,0)	527, 556	528, ---	---, ---
(4,0)	945, 1151	---, ---	950, ---

Table 1. Comparison of measured frequencies

4 DISCUSSION

Given that the ESPI and SLDV methods use different approaches it is very encouraging that the results are in such reasonable agreement. For the ESPI work the gong was excited acoustically with a sinusoidal signal whose frequency was varied manually and tuned in to find the amplitudes' peaks. This introduced uncertainties into the resonant frequency value as the peaks were sometimes rather broad. It also made the experiments long and tedious. SLDV on the other hand excited the gong mechanically with "white noise" and the frequencies were extracted by the software. However, it could also take a very long time to complete a run but has the advantage of being essentially automated. ESPI was more sensitive as a detector of modes and produced numerous harmonics and subharmonics of true modes. Although the interpretation of the ESPI interferograms was difficult when looking at the gong's rim, it was possible to do so successfully.

With SLDV looking at the shoulder and, especially, the rim was problematic. This could be attributed to a number of things including a sub-optimal choice of driving point and/or the fact that in this SLVD experiment burst random excitation was used to simultaneously excite all modes with a significantly lower input energy per mode. This reduced energy per mode may also account for the absence of harmonics and other non-linear effects.

The reliability of the SLDV technique described has been determined and work on a series of gongs from the same gamelan is being carried out and will be the subject of a later paper.

5 REFERENCES

1. R. Perrin and T. Charnley, Group theory and the bell, J. Sound Vib., 31, 411-418 (1973).
2. N. Herington, D.P. Elford, G.M. Swallowe, L. Chalmers, R. Perrin and T.R. Moore, Normal modes of a gamelan gong, Proc. 1st EAA-EuroRegio Congress on Acoustics & Vibration, Paper number 165. Ljubljana (2010).
3. R. Perrin, L. Chalmers, D.P. Elford, G.M. Swallowe and T.R. Moore, Normal modes of the Indian elephant bell, J.A.S.A., 131(3) 2288-2294. (2012).
4, T.D. Rossing, Science of Percussion Instruments, World Scientific, 98-99, (2000).
5. J.R. Bell and S.J. Rothberg, Laser vibrometers and contacting transducers, target rotation and six degree-of-freedom vibration: what do we really measure?, J. Sound Vib. 237(2), 245-261 (2000).
6. S.J. Rothberg, B.J. Halkon, M. Tirabassi and C. Pusey, Radial vibration measurements directly from rotors using laser Vibrometry: the effects of surface roughness, instrument misalignments and pseudo-vibration, Mech. Syst. & Signal Process. 33(11) 109-131 (2012).